Available online at www.worldscientificnews.com

World Scientific News

WSN 52 (2016) 44-56 EISSN 2392-2192

Comparison of the Hydrodynamics for Pressure – Driven and Acceleration – Driven Poiseuille flow

Alalibo T. Ngiangia

Department of Physics, University of Port Harcourt,
P M B 5323, Choba, Port Harcourt, Nigeria

E-mail address: kellydap08@gmail.com , alalibo.ngiangia@uniport.edu.ng

ABSTRACT

A study on the comparison of the pressure-driven Poiseuille flow and acceleration-driven Poiseuille flow was made by analyzing the resulting models of the flow configuration. It is shown that at the hydrodynamic level, there exist a difference in magnitude of the two flows but at the microscopic level the body force and the pressure gradient which are the driving forces are different due to spatial variations in the both flows.

***Keywords*:** Poiseuille flow. Pressure-driven; Acceleration-driven; Hydrodynamics; Cylindrical coordinate

PACS: 47.85.L-

1. INTRODUCTION

The concept of Poiseuille flow started with the work of Poiseuille [1] and also independently by Hagen [2] and interchange with the name Hagen-Poiseuille flow. The assumptions of the equation derived are that the fluid is incompressible and Newtonian, the flow is laminar through a pipe of constant circular cross section that is substantially longer than its diameter and there is no acceleration of fluid in the pipe. Poiseuille fluid flow is

confined between two rigid parallel plates that are stationary and act as thermal reserviours. It is a physical law that gives the pressure drop in an incompressible and Newtonian fluid in laminar flow flowing through a long cylindrical pipe of constant cross section. It can be applied to air flow in lung alveoli, drinking straw or hypodemic needle. Its application in blood flow, drainages and refining of petroleum products in a fractionating column cannot be overemphasized. Studies of Poiseuille flow has been extensively dealt with by researchers, Walton [3], in his study, shows that no neutral solution exist if a combination of the axial and azimuthal wave numbers of the perturbation exceeds a critical value. As a consequence, the physical problem admits only neutral solutions for an azimuthal wave number.

Zheng et al. [4], carried out a study of kinetic and hydrodynamics for Poiseuille flow in rectangular coordinate system using numerical methods for the Navier-Stokes equation and direct simulation Monte Carlo simulation and reported useful findings. Ngiangia and Wonu [5], Ngiangia [6], Ngiangia et al [7], Orukari et al. [8], Friggard and Nouar [9] and Ngiangia and Orukari [10] all dealt with Poiseuille flow with its affecting parameters and reported findings that enrich the literature of the fluid flow. Zammert and Eckhardt [11], applied the edge tracking method to plane Poiseuille flow in sub-critical state (Re < 5772) and calculated the edge state over a wide range of Reynolds number (Re) (2000-4200), thereby identifying the exact coherent state. Our aim in this study is to investigate the pressure-driven and acceleration-driven Poiseuille flow in cylindrical coordinate and compare their velocity, temperature and pressure relationship. This in our view will expand and extend the work of Zheng et al. [4] and Corenflos et al. [13].

Nomenclature

α = flow behaviour index (power law exponent)
R = universal fluid constant
ρ = fluid density
P = fluid pressure
φ = consistency index
u = fluid velocity
a = thermal diffusivity
r = radius of the cylinder
C_V = specific heat at constant volume
μ = absolute viscosity
T = fluid temperature
t = time
Φ = dissipation function (viscous heating

2. FORMALISM

The governing hydrodynamic equations for describing Plane Poiseuille flow in cylindrical coordinate are:

$$\frac{1}{r}\frac{\partial}{\partial r}(ru)=0 \tag{1}$$

$$\frac{\partial u}{\partial t}=\frac{\mu}{\rho}\left[\frac{\partial^2 u}{\partial r^2}+\frac{1}{r}\frac{\partial u}{\partial r}-\frac{u}{r^2}\right]+B-\frac{1}{\rho}\frac{\partial P}{\partial r} \tag{2}$$

$$\frac{\partial T}{\partial t}=-a\left[\frac{\partial^2 T}{\partial r^2}+\frac{1}{r}\frac{\partial T}{\partial r}\right]+\frac{\Phi}{\rho C_V}-\frac{P}{\rho C_V}\frac{\partial u}{\partial r} \tag{3}$$

The equation of state for an ideal fluid is given by

$$P=\rho RT \tag{4}$$

It has been established by Hughes and Brighton [12] that

$$\varphi\left(-\frac{\partial u}{\partial r}\right)^{\alpha}=-\frac{r}{2}\left(\frac{\partial p}{\partial r}\right) \tag{5}$$

Subject to the initial and boundary conditions

$$u\left(\frac{1}{2}\right)=U. \qquad u\left(-\frac{1}{2}\right)=0 \tag{6}$$

$$T\left(\frac{1}{2}\right)=0 \qquad T\left(-\frac{1}{2}\right)=1 \tag{7}$$

3. METHOD OF SOLUTION

For the pressure-Driven case and for Newtonian fluid $(\alpha=1)$, we use (5) and (4) in (3) and transform the resulting equation using the expressions

$$u=u_1(r)e^{-\lambda t} \tag{8}$$

$$T=T_1(r)e^{-\lambda t} \tag{9}$$

$$\Phi=\Phi_1(r)e^{-\lambda t} \tag{10}$$

where λ is a constant into

$$\left[\frac{d^2T_1(r)}{dr^2}+\frac{1}{r}\frac{dT_1(r)}{dr}\right]-\beta_3 T_1(r)+\beta_1\frac{dT_1(r)}{dr}=\beta_2 \tag{11}$$

where $\beta_1 = \frac{PR}{2\rho C_V a}$, $\beta_2 = \frac{\Phi_1}{a\rho C_V}$, $\beta_3 = \frac{\lambda}{a}$

Subject to the initial and boundary conditions

$$T_1\left(\frac{1}{2}\right) = 0 \qquad T_1\left(-\frac{1}{2}\right) = e^{\lambda t} \tag{12}$$

$$u_1\left(\frac{1}{2}\right) = Ue^{\lambda t} \qquad u_1\left(-\frac{1}{2}\right) = 0 \tag{13}$$

The approximate solution of (11) with the imposition of (12), and using (9) as well as (10), we get

$$T(r) = a_0\left(1 + \frac{\beta_3}{4}r^2 + \frac{\beta_3(\beta_3 - 2\beta_1)}{64}r^4\right) + a_1\left(r + \left(\frac{\beta_3 - \beta_1}{9}\right)r^3 + \left(\frac{(\beta_3 - \beta_1)(\beta_3 - 3\beta_1)}{225}\right)r^5\right) - \frac{\beta_2}{\beta_3} \tag{14}$$

where:

$$\Phi_1 = \Phi \text{ in } \beta_2, \quad a_1 = \frac{\beta_3 + \beta_2 + r_{13}\beta_2}{\beta_3(r_{14} - r_{12}r_{13})}, \quad a_0 = \frac{r_{12}\beta_2 + \beta_2 r_{14} - r_{12}\beta_3 - 2\beta_2 r_{12} r_{13}}{r_{11}\beta_3(r_{14} - r_{12}r_{13})}$$

$$r_{11} = \left(1 + \frac{\beta_3}{16} + \frac{\beta_3(\beta_3 - 2\beta_1)}{1024}\right) = r_{13}, \quad r_{12} = \left(-\frac{1}{2} - \frac{(\beta_3 - \beta_1)}{72} - \frac{(\beta_3 - \beta_1)(\beta_3 - 3\beta_1)}{7200}\right)$$

$$r_{14} = \left(\frac{1}{2} + \frac{(\beta_3 - \beta_1)}{72} + \frac{(\beta_3 - \beta_1)(\beta_3 - 3\beta_1)}{7200}\right)$$

Similarly, using (5), (2) can be rewritten as

$$\frac{\partial u}{\partial t} = \frac{\mu}{\rho}\left[\frac{\partial^2 u}{\partial r^2} + \frac{1}{r}\frac{\partial u}{\partial r} - \frac{u}{r^2}\right] + B - \frac{2\varphi}{\rho r}\frac{\partial u}{\partial r} \tag{15}$$

Using the transformation

$$B = B_1(r)e^{-\lambda t} \tag{16}$$

and that of (8), (15) is transformed and its approximate solution after the imposition of (13) is

$$u(r)=b_0\left(1-\frac{\alpha_1}{5-2\alpha_3}r^2+\frac{\alpha_1^2}{(5-2\alpha_3)(17-4\alpha_3)}r^4+.....\right)+$$
$$b_1\left(r-\frac{\alpha_1}{10-3\alpha_3}r^3+\frac{\alpha_1^2}{(10-3\alpha_3)(25-5\alpha_3)}r^5+.....\right)-\frac{B}{\lambda} \quad (17)$$

where:

$$b_1=\frac{\varphi_2\chi_1-\varphi_1\chi_3}{\chi_4\chi_1-\chi_2\chi_3},\quad b_0=\frac{\varphi_1\chi_4\chi_1-\varphi_2\chi_1\chi_2}{(\chi_4\chi_1-\chi_3\chi_2)\chi_1},$$
$$\chi_1=\left(1-\frac{\alpha_1}{20-8\alpha_3}+\frac{\alpha_1^2}{16(5-2\alpha_3)(17-4\alpha_3)}=\chi_3\right),$$

$$\chi_2=\left(\frac{1}{2}-\frac{\alpha_1}{80-24\alpha_3}+\frac{\alpha_1^2}{32(10-3\alpha_3)(25-5\alpha_3)}\right),$$
$$\chi_4=\left(\frac{1}{2}+\frac{\alpha_1}{80-24\alpha_3}-\frac{\alpha_1^2}{32(10-3\alpha_3)(25-5\alpha_3)}\right)$$

$$\varphi_1=U+\frac{B}{\lambda},\quad \varphi_2=\frac{B}{\lambda},\ \alpha_1=\frac{\rho\lambda}{\mu},\ \alpha_3=\frac{2\varphi}{\mu}$$

The shear stress is given as

$$\varsigma_r=\mu\left(\frac{du}{dr}-\frac{u}{r}\right)= \mu b_0\left(\frac{2\alpha_1}{5-2\alpha_3}r+\frac{4\alpha_1^2}{(5-2\alpha_3)(17-4\alpha_3)}r^3+.....\right)+$$
$$\mu b_1\left(1-\frac{3\alpha_1}{10-3\alpha_3}r^2+\frac{5\alpha_1^2}{(10-3\alpha_3)(25-5\alpha_3)}r^4+.....\right)$$

$$-\mu b_0\left(\frac{1}{r}-\frac{\alpha_1}{5-2\alpha_3}r+\frac{\alpha_1^2}{(5-2\alpha_3)(17-4\alpha_3)}r^3+.....\right)+$$
$$\mu b_1\left(1-\frac{\alpha_1}{10-3\alpha_3}r^2+\frac{\alpha_1^2}{(10-3\alpha_3)(25-5\alpha_3)}r^4+.....\right)-\frac{B}{\lambda r} \quad (18)$$

The Nusselt number is

$$Nu=k_T\left(\frac{dT}{dr}-\frac{T}{r}\right) = k_T a_0\left(\frac{\beta_3}{4}r+\frac{\beta_3(\beta_3-2\beta_1)}{16}r^3\right)+$$
$$k_T a_1\left(1+\left(\frac{\beta_3-\beta_1}{3}\right)r^2+\left(\frac{(\beta_3-\beta_1)(\beta_3-3\beta_1)}{45}\right)r^4\right)$$

$$k_T a_0\left(\frac{1}{r}+\frac{\beta_3}{4}r+\frac{\beta_3(\beta_3-2\beta_1)}{64}r^3\right)+$$
$$-k_T a_1\left(r+\left(\frac{\beta_3-\beta_1}{9}\right)r^2+\left(\frac{(\beta_3-\beta_1)(\beta_3-3\beta_1)}{225}\right)r^4\right)-\frac{\beta_2}{\beta_3 r} \quad (19)$$

3. 1. Acceleration- driven case

The pressure –driven flow is related to the acceleration-driven case because a constant pressure gradient will serve as a constant body force (acceleration). The implication of this assertion is that the body force B, and the pressure gradient in (2) are equivalent at the hydrodynamic level. Also $\frac{\partial u}{\partial r}=0$ (the last term of equation (3)), hence our governing equations of (2) and (3) reduce to

$$\frac{\partial u}{\partial t}=\frac{\mu}{\rho}\left[\frac{\partial^2 u}{\partial r^2}+\frac{1}{r}\frac{\partial u}{\partial r}-\frac{u}{r^2}\right]-\frac{2}{\rho}\frac{\partial P}{\partial r} \quad (20)$$

$$\frac{\partial T}{\partial t}=-a\left[\frac{\partial^2 T}{\partial r^2}+\frac{1}{r}\frac{\partial T}{\partial r}\right]+\frac{\Phi}{\rho C_V} \quad (21)$$

Following the same procedure, the approximate solution of (21) is given by

$$T(r)=C_0\left(1+\frac{\lambda}{4a}r^2+\frac{\left(\frac{\lambda}{a}\right)^2}{64}r^4\right)+C_1\left(r+\frac{\lambda}{9a}r^3+\frac{\left(\frac{\lambda}{a}\right)^2}{225}r^5\right)-\frac{\Phi}{\lambda} \quad (22)$$

where:

$$C_0=\frac{e_{13}e_{14}+e_{12}e_{15}}{e_{11}(e_{12}-e_{14})},\quad C_1=\frac{e_{13}-e_{15}}{e_{12}-e_{14}},\quad e_{11}=\left(1+\frac{\lambda}{16a}+\frac{\left(\frac{\lambda}{a}\right)^2}{1024}\right)$$

$$e_{12}=\left(-\frac{1}{2}-\frac{\lambda}{72a}-\frac{\left(\frac{\lambda}{a}\right)^2}{7200}\right),\quad e_{13}=\frac{\Phi}{\lambda},\quad e_{14}=\left(\frac{1}{2}+\frac{\lambda}{72a}+\frac{\left(\frac{\lambda}{a}\right)^2}{7200}\right),\quad e_{15}=1+\frac{\Phi}{\lambda}$$

Using (5), (20) can be written as

$$\frac{\partial u}{\partial t}=\frac{\mu}{\rho}\left[\frac{\partial^2 u}{\partial r^2}+\frac{1}{r}\frac{\partial u}{\partial r}-\frac{u}{r^2}\right]-\frac{4\varphi}{\rho r}\frac{\partial u}{\partial r} \tag{23}$$

The solution of (21) following the usual procedure for the pressure-driven case is

$$u(r)=d_0\left(1-\frac{\alpha_{11}}{2-\alpha_{22}}r^2+\frac{\alpha_{11}^2}{(2-\alpha_{22})(6-\alpha_{22})}r^4\right)+ d_1\left(r-\frac{\alpha_{11}}{4-3\alpha_{22}}r^3+\frac{\alpha_{11}^2}{(4-3\alpha_{22})(8-5\alpha_{22})}r^5\right) \tag{24}$$

where:

$$f_{11}=\left(1-\frac{\alpha_{11}}{8-4\alpha_{22}}+\frac{\alpha_{11}^2}{16(2-\alpha_{22})(6-\alpha_{22})}\right),\ f_{12}=\left(\frac{1}{2}-\frac{\alpha_{11}}{8(4-3\alpha_{22})}+\frac{\alpha_{11}^2}{32(4-3\alpha_{22})(8-5\alpha_{22})}\right)$$

$$f_{13}=\left(-\frac{1}{2}+\frac{\alpha_{11}}{8(4-3\alpha_{22})}-\frac{\alpha_{11}^2}{32(4-3\alpha_{22})(8-5\alpha_{22})}\right),\ d_0=\frac{-Uf_{13}}{f_{11}(f_{12}-f_{13})},\ d_1=\frac{U}{f_{12}-f_{13}}$$

$$\alpha_{11}=\frac{\rho\lambda}{\mu},\ \ \alpha_{22}=\frac{4\varphi}{\mu}$$

$$\varsigma_r=\mu\left(\frac{du}{dr}-\frac{u}{r}\right)= \begin{array}{l}\mu d_0\left(-\frac{2\alpha_{11}}{2-\alpha_{22}}r+\frac{4\alpha_{11}^2}{(2-\alpha_{22})(6-\alpha_{22})}r^3\right)+\\ \mu d_1\left(1-\frac{3\alpha_{11}}{4-3\alpha_{22}}r^2+\frac{5\alpha_{11}^2}{(4-3\alpha_{22})(8-5\alpha_{22})}r^4\right)\end{array}$$

$$- \begin{array}{l}\mu d_0\left(\frac{1}{r}-\frac{\alpha_{11}}{2-\alpha_{22}}r+\frac{\alpha_{11}^2}{(2-\alpha_{22})(6-\alpha_{22})}r^3\right)+\\ \mu d_1\left(1-\frac{\alpha_{11}}{4-3\alpha_{22}}r^2+\frac{\alpha_{11}^2}{(4-3\alpha_{22})(8-5\alpha_{22})}r^4\right)\end{array} \tag{25}$$

$$Nu=k_T\left(\frac{dT}{dr}-\frac{T}{r}\right)=k_T C_0\left(\frac{\lambda}{2a}r+\frac{\left(\frac{\lambda}{a}\right)^2}{16}r^3\right)+k_T C_1\left(1+\frac{\lambda}{3a}r^2+\frac{\left(\frac{\lambda}{a}\right)^2}{45}r^4\right)$$

$$-k_T C_0\left(\frac{1}{r}+\frac{\lambda}{4a}r+\frac{\left(\frac{\lambda}{a}\right)^2}{64}r^3\right)+k_T C_1\left(1+\frac{\lambda}{9a}r^2+\frac{\left(\frac{\lambda}{a}\right)^2}{225}r^4\right)-\frac{\Phi}{\lambda r} \qquad (26)$$

Table 1. Readings of temperature for pressure-driven and acceleration-driven cases.

	Temp for P-D (T)	Temp for A-D (T)
0	0.0000001408	-371.064
1	0.00302004	-371.063
2	0.0060008	-369,060
3	0.00906028	-368.053
4	0.01208o6	-367.093
5	0.0151011	-366.017

Table 2. Readings of velocity for pressure-driven and acceleration-driven cases.

r	Velocity for P-D (u)	Velocity for A-D (u)
0	-19.0583	2.14657
1	808758	7.67537
2	12807200	23.02080
3	64163300	66.55410
4	200660000	175.31600
5	484698000	412.67600

Table 3. Readings of pressure for pressure-driven and acceleration-driven cases.

r	Pressure for P-D (P)	Pressure for A-D (P)
0	0.00	0.00
1	3668800	11.80130

2	29058700	46.48230
3	97113400	105.63900
4	227929000	211.44000
5	440755000	391.11400

Table 4. Readings of Shear stress for pressure-driven and acceleration-driven cases

r	Shear stress for P-D (s)	Shear stress for A-D (s)
0	0.998891	743.827
1	0.68553	371.412
2	0.843427	186.646
3	0.898986	126.659
4	o.930436	98.6016
5	0.954896	83.9112

Table 5. Readings of Nusselt number for pressure-driven and acceleration-driven cases.

r	Nusselt number for P-D (Nu)	Nusselt number for A-D (Nu)
0	0	0
1	-349664	0.0000048972
2	-0.00000511666	0.00000039155
3	-0.00000104992	0.0000000132147
4	-0.00000140047	0.0000000313233
5	-0.00000175157	0.0000000611774

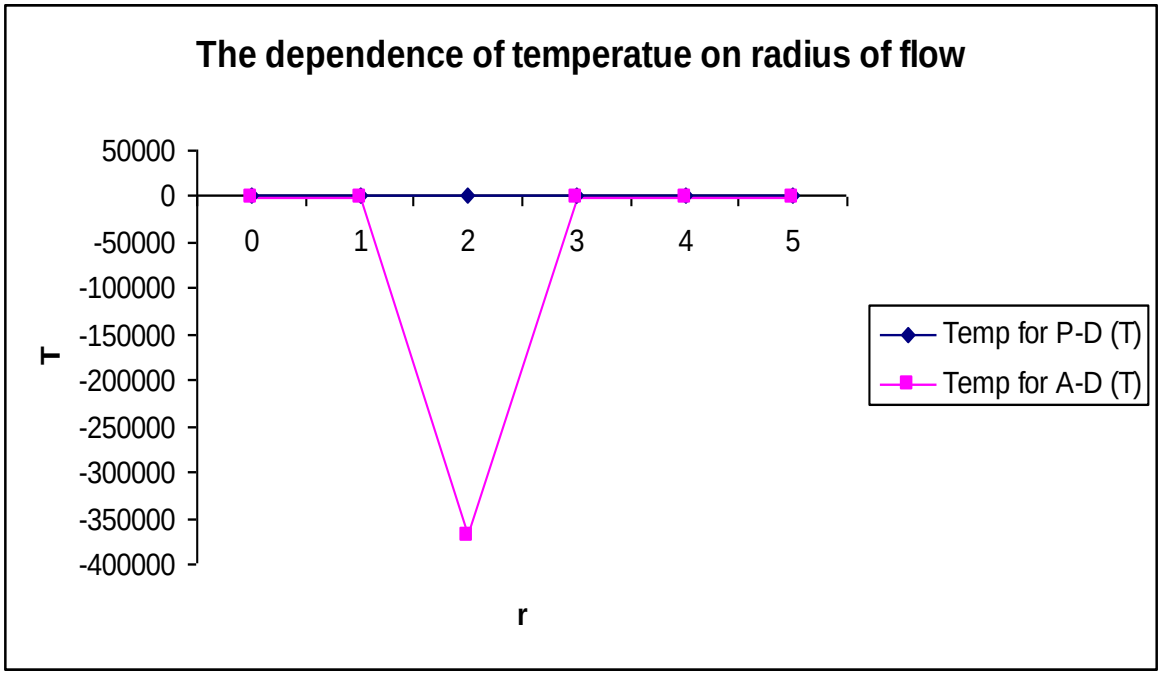

Figure 1. Showing variation of Temperature on increasing radius of flow.

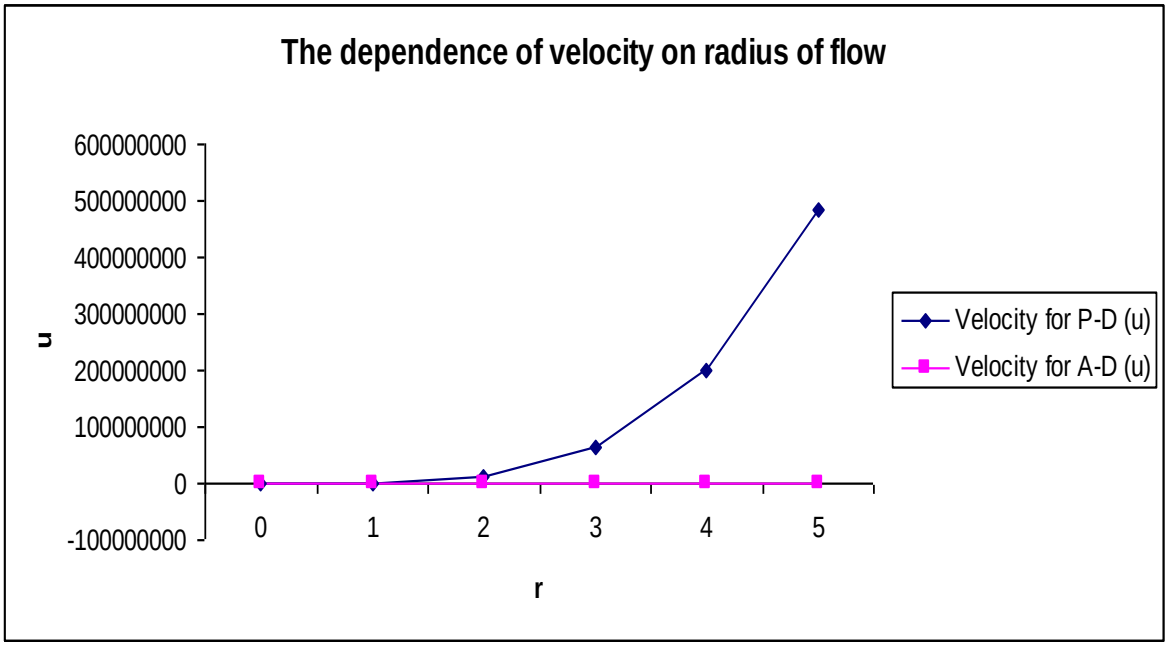

Figure 2. Showing variation of velocity profile on increasing radius of flow

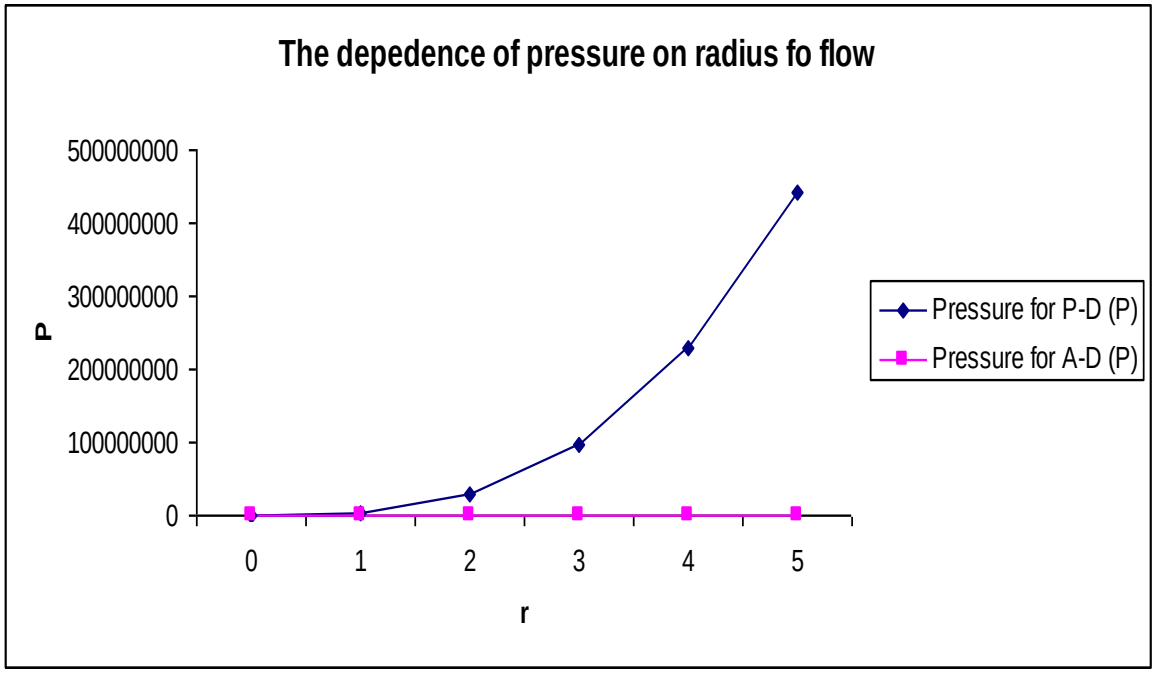

Figure 3. Showing variation of pressure profile on increasing radius of flow.

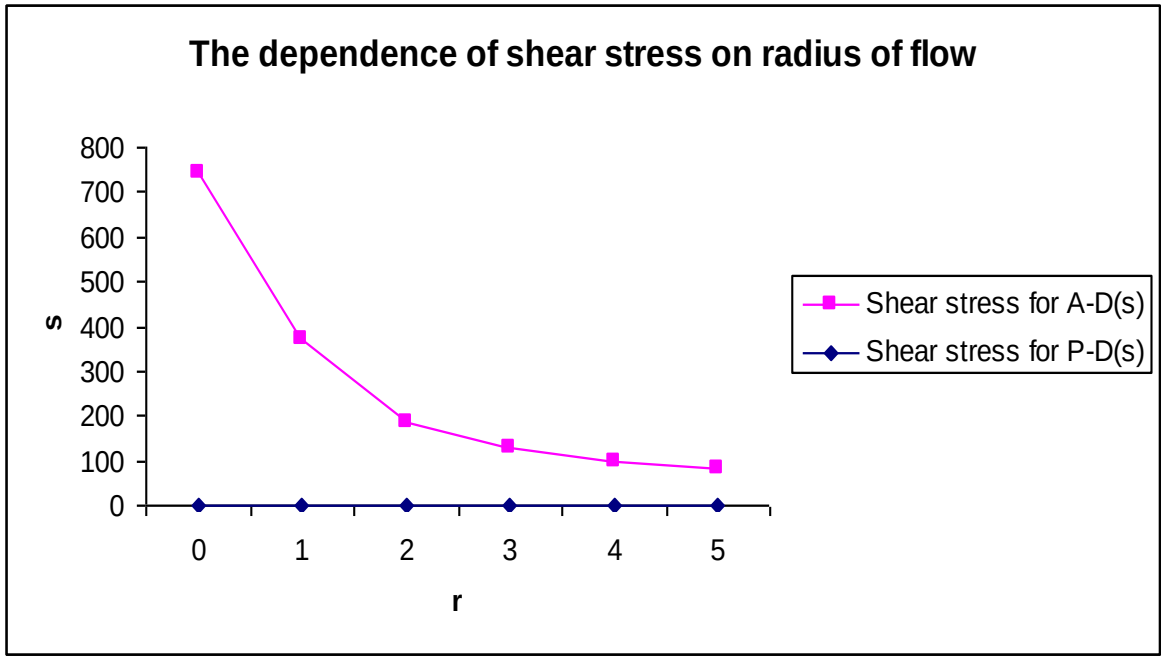

Figure 4. Showing variation of shear stress on increasing radius of flow.

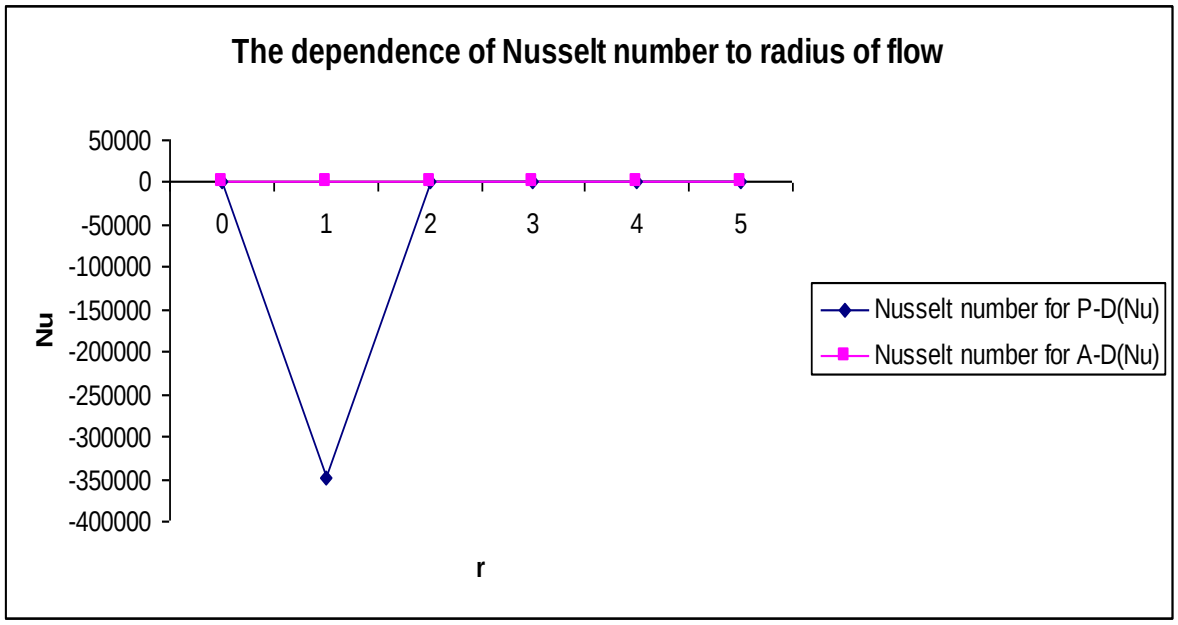

Figure 5. Showing variation of Nusselt number on increasing radius of flow.

5. RESULTS AND DISCUSSION

In order to get physical insight and numerical validation of the problem, a typical value of universal fluid constant 8.31 and fluid density of water 1000 is chosen. The values of other parameters made use of are

$$a = 1.2, R = 8{,}31, \rho = 1000, \Phi = 1.3, \varphi = 1.7, B = 0.8, C_V = 4200, U = 3.6, P = 1,$$
$$\mu = 0.001, \lambda = 0.0035$$

,

Comparison of the pressure-driven case and the acceleration-driven case as shown in Figure 1 reveals that for the pressure-driven Poiseuille flow, there exist a cooling by expansion particularly when the flow is compressible, brought about by the presence of $\frac{\partial u}{\partial r}$ in equation (3). This cooling term is absent and the presence of the viscous function term in the acceleration-driven Poiseuille flow has no hindrance to its heating hence the difference in the shape of the two curves.

For Figure 2, at the microscopic level, the two driving forces are very different since an external forces accelerate individual particles while a pressure gradient induces a combined flow due to spatial variation of the particles for the pressure driven case but for the acceleration driven case, the body force B and the pressure gradient $\frac{\partial P}{\partial r}$ are equivalent at the hydrodynamic level hence the different shape of the two curves. For the pressure-driven and acceleration driven cases as shown in Figure 3, the same prevailing conditions exist as in Figure 2.

The shear stresses of the pressure driven case and that of the acceleration driven case as depicted in Figure 4 clearly shows the differences in the two flows at both the macroscopic level and the microscopic level, the nature of the viscosity of the fluid not affecting the distinction. The Nusselt number (heat transfer coefficient) between the two flows as shown in Figure 5 also laid credence to the difference between two flows often ignored by researchers but very important because attempting to describe the two flows as the same may lead to wrong formulation of flow models in this fluid flow configuration.

6. CONCLUSION

Pressure-driven Poiseuille flow and acceleration-driven Poiseuille flow are governed by two different models. Although, at the hydrodynamic level, the difference is only in magnitude for the acceleration-driven case as shown in equations (20) and (21) while that of the pressure-driven case is different as shown in equations (2) and (3). The shear stress and the heat transfer coefficient also shed light on the two models.

References

[1] J L M Poiseuille, *C. R. Acad Sci* 11, 961 (1839).
[2] G Hagen, *Pogg. Ann* 46, 423 (1840).
[3] A G Walton, *Studies in Applied Math* 106, 315 (2001).
[4] Y Zheng, A L Garcia, and B J Alder, *Jour. of Stat. Phys* 109, 314 (2002)
[5] A T Ngiangia and N Wonu, *Jour. of Applied Sci. and Env. Manag (JASEM)* 11(2), 209 (2007).
[6] A T Ngiangia, *J of NAMP* 11, 87 (2007).
[7] A T Ngiangia, N Ojekudo, O Amadi and M A Orukari, *J of Math. Assoc. of Nig. (ABACUS)* 38(2), 1 (2011).
[8] M A Orukari, A T Ngiangia and F Life-George, *J of NAMP* 18, 201 (2011).
[9] I Friggard and C Nouar *Phys of Fluids* 15(10), 2843 (2003).
[10] A T Ngiangia and M A Orukari *Global Jour. of Pure and Applied Math* 9(2), 169 (2013).
[11] S Zammert and B Eckhardt, *Fluid Dyn. Res. IOP publishing* 46(4), 041419 (2014).
[12] W F Hughes and J A Brighton, *Fluid Dynamics* (New York: *Third edition Schaum's Outlines, McGraw-Hill*) Ch 12, Sec 3, P 308 (1999).
[13] S K Corenflos, S Rida, J C Mormier, P Dupont, K Dangtram and M Stannislas, *Proc. Inter. Symp. on refined flow model. and turb. Measu.* 499 (1993).

(Received 28 June 2016; accepted 12 July 2016)